Article:
Francis, MJ orcid.org/0000-0002-7033-7368, Glover, ZJ, Yu, Q et al. (2 more authors) (2019) Acoustic characterisation of pH dependant reversible micellar casein aggregation. Colloids and Surfaces A: Physicochemical and Engineering Aspects, 568. pp. 259-265. ISSN 0927-7757

https://doi.org/10.1016/j.colsurfa.2019.02.026

Acoustic characterisation of pH dependant reversible micellar casein aggregation

M. J. Francis[1*], Z. J. Glover[1&2], Q. Yu[1], M. J. Povey[1], M. J. Holmes[1]

1 School of Food Science and Nutrition, University of Leeds, Leeds, LS2 9JT, United Kingdom
2 Department of Physics, Chemistry and Pharmacy, University of Southern Denmark, Campusvej 55, 5230, Odense, Denmark

*Corresponding Author: M.Francis1@leeds.ac.uk

Abstract

Ultrasound and light-based measurements were used to monitor changes in agitated and quiescent solution characteristics such as particle size distribution during casein aggregation and redistribution in a model colloidal system. The precipitation of casein micelles was controlled by adjusting the pH of the solution to alter the stability of the micelles. The studied dispersions were prepared at high pH, taken through the isoelectric point to precipitate and then re-dispersed by further lowering the pH at specific intervals. The isoelectric point was determined by zeta potential measurement at each specific pH interval. The isoelectric point of the casein dispersions was in the region of pH 4.3-4.7. Changes in the particle size of this reversible casein system were successfully measured acoustically. The dissolution rate and solution kinetics were subsequently monitored in a wide pH range using a combination of acoustic and light-based methods.

Keywords
Acoustic spectroscopy, ultrasound, casein, aggregation.

Introduction

Many dynamic colloidal mechanisms occur during food processing, all of which effect the structural properties of the final product. Acoustic based techniques offer dynamic in-situ measurements that can characterise such mechanisms including aggregation, precipitation, gelation and crystallisation. These processes often form the structural base of products including cheese (aggregation/gelation) [1,2], yoghurt (aggregation/ precipitation/ gelation) [1,3,4], cream cheese (precipitation) [5,6], butter (crystallisation) [7,8], bread (gelation/crystallisation) [9,10], and chocolate (crystallisation) [11,12]. These complex systems can be difficult to characterise, even for seemingly simple parameters such as particle size. A detailed understanding of the processes involved in such colloidal mechanisms can be gained by using a well-defined model system which can evaluate the efficacy of the available analytical toolkit and provide the basis for data interpretation in more complex multi-component systems.

Micellar casein is ubiquitous in many food products, most notably forming the main structural element of fermented dairy products [13,14]. In bovine milk, caseins comprise 80 % of the total protein fraction (~3-5 % of fresh milk w/w) and are comprised of 4 monomeric phosphoprotein units [15]. These protein molecules contain a high degree of negatively charged phosphate groups on their amino acid backbone,

which are calcium sensitive. Three monomeric units, α_{S1}, α_{S2} and β casein form the structural centre of the micelle, whilst κ-casein is found at the surface [16]. κ-casein contains a glycosylated electronegative motif on the C-terminal which forms a hairy layer at the surface of the micelle [17] leading to steric and electrostatic stabilisation at native pH (pH 6.7) [18]. The internal structure of the micelle is held together through a combination of hydrogen bonding, hydrophobic interactions and ionic bonding mediated through the presence of calcium phosphate nano-crystals [19].

Micellar casein has a particle size distribution from 50 – 600 nm in diameter with an average of 150 nm [20,21] and can be manipulated to aggregate and re-disperse by controlling the pH [22], therefore, providing a model system to monitor changes in effective particle size distribution. The isoelectric point, the pH at which a protein has a net charge of zero, is 4.5-4.8 for micellar casein [23,24]. At a pH above the isoelectric point, casein will have a net negative charge due to ionisation of the acidic side chains. Therefore, casein is soluble in dilute sodium hydroxide solution. At a pH below the isoelectric point, casein will have a net positive charge due to protonation of the basic side chains making casein soluble in strongly acidic solutions. At pH values around the isoelectric point, casein micelles will have a net charge of zero and will begin to aggregate following loss of steric repulsion due to the collapse of the stabilising hairy layer of κ-casein and removal of the electrostatic repulsion between micelles.

Casein micelles can become completely dissociated when dispersed in highly alkaline solutions [25,26]. However, it has been demonstrated that micelles can be reformed through a subsequent reduction in pH with a roughly 10% reduction in zeta potential and average particle size [27]. This will not affect the results of this study as the casein micelles are being used as a reversible aggregation system controlled through pH cycling. The cycling of pH will also cause irreversible alterations of the ionic content and structure within the casein micelles, however in the context of this model this is irrelevant, as only changes in effective particle size, and not mechanical properties or future functionality are considered. Micellar integrity is maintained when calcium phosphate 'glue' is removed by acidification, suggesting additional principal stabilisation is provided by casein-casein interactions [28]. The casein micelle system was chosen as the model system for this study due to the ability to control the aggregation of the micelles by altering the pH. A schematic of the micelles at the isoelectric point and at a pH above and below the isoelectric point is presented in Figure 1.

Two common measurement methods used to study precipitating/aggregating solutions are Dynamic Light Scattering (DLS), for determining the particle size of aggregates, [29–31] and turbidity/transmission of light, to monitor either nucleation events [32–34] or the formation of aggregates [35–37]. These measuring techniques are commonly used to study dairy systems [38–40]. However, both measurement techniques have limitations. DLS requires particles to be within a certain size range (0.3 nm-10 μm) and polydisperse particles can be difficult to measure as larger particles are generally overestimated at the expense of smaller particles [41–43]. Turbidity measurements are limited by cost, measurement repeatability and the fragility of sensors [44–46].

Acoustic methods are repeatable, non-destructive, non-invasive and can measure concentrated and polydisperse systems [47–49]. Ultrasonic techniques can reliably

size particles between 10 nm and 1 mm [50]. Acoustic techniques have been effectively used to study casein micelles in suspension. Ultrasonic attenuation measurements have been used to determine the behaviour of casein micelles in milk fractions [51] and to estimate the particle size [52,53] and zeta potential [54] of casein micelles. Ultrasonic velocity measurements have also been used to monitor calcium dissociation from casein micelles [55], gel formation involving casein micelles [56,57], casein concentration in skim milk [58], the phase separation of casein [59] and the stability of emulsions using casein as an emulsifier [60]. Two different ultrasound methods were used in this study: Acoustic Attenuation Spectroscopy (Malvern Ultrasizer) and Ultrasound Reflectance Spectroscopy (Crystal Stik).

The Malvern Ultrasizer MSV is a commercial Acoustic Attenuation Spectroscopy (AAS) instrument that can measure acoustic attenuation between 2 and 120 MHz to within ±0.04 dB cm^{-1} [52]. The Ultrasizer uses a pair of low and high frequency transducers in a pitch/catch arrangement to measure the absolute attenuation. The measurement principle of the Ultrasizer is shown in Figure 1. The Ultrasizer can measure solutions with concentrations ranging from 0.5 to 50 volume percent, without dilution, with a measurable size range from 0.01 µm to 1000 µm [61]. The Ultrasizer can give an accurate in-situ representation of solution characteristics and kinetics for industrially relevant compositions.

The Ultrasizer determines the relationship between frequency and attenuation. The resulting attenuation spectra is inverted to a particle size distribution and volume fraction using a mathematical model based on single particle scattering theory referred to as ECAH (Epstein, Carhart, Allegra and Hawley) theory [62]. Particle size is reported as the volume mean diameter denoted D_{43} (nm). It should be noted that particle size determined from DLS intensity measurements are often greater than those reported as D_{43} due to the calculation process. In addition, during measurement constant agitation (500 rpm) takes place to reduce thermal fluctuations. This feature also affects the aggregation behaviour of the samples when undergoing destabilisation during pH changes.

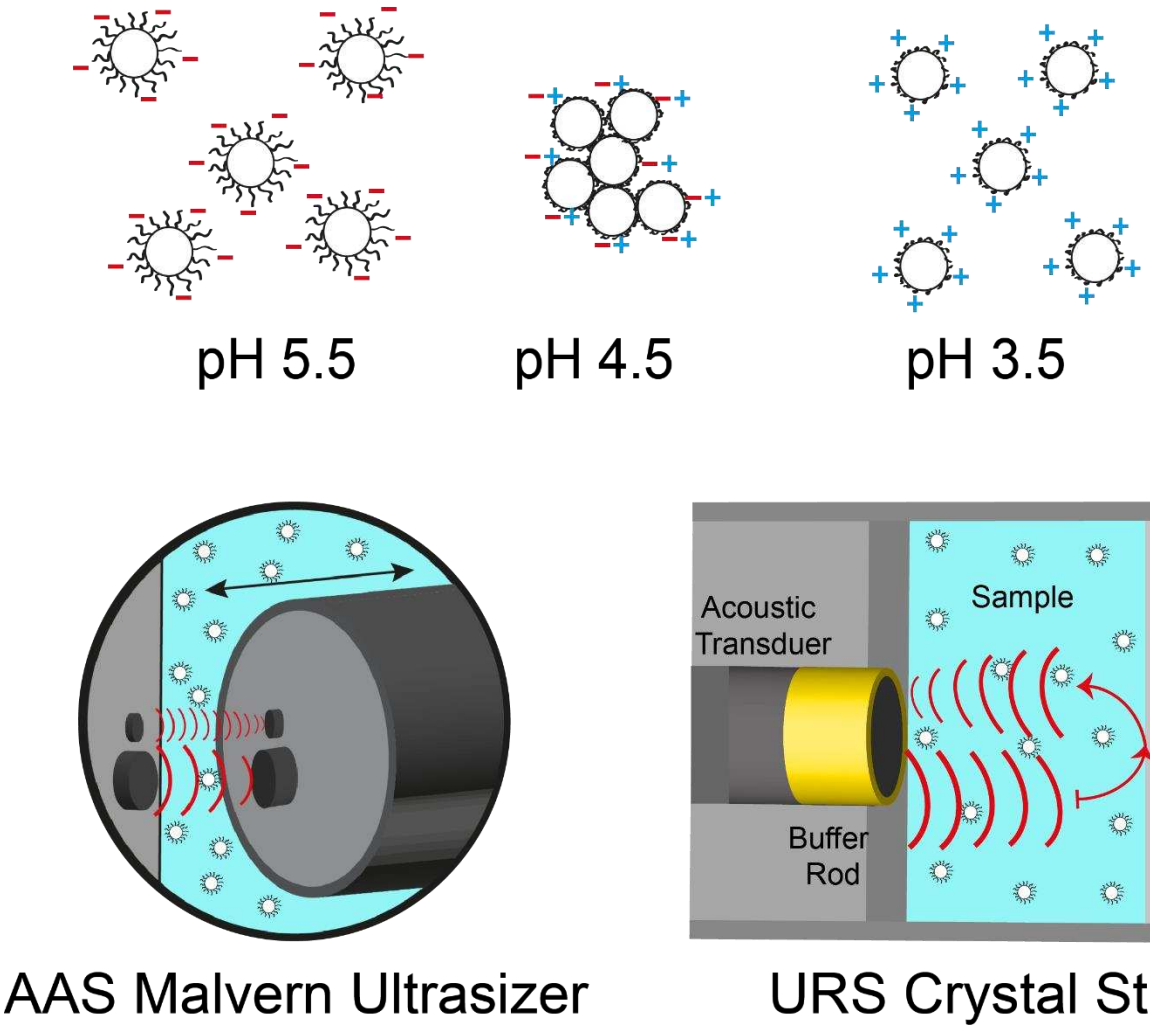

Figure 1: Schematic demonstrating reversible model casein micelle system and the two acoustic techniques used to interrogate the samples.

Ultrasound Reflectance Spectroscopy (URS) is a well-established technique used for the characterisation of different materials [63–66]. Unlike the Malvern Ultrasizer which operates in a pitch-catch arrangement, URS operates in a pulse-echo mode with the pulse travelling through a buffer rod then the sample before reflecting and being collected by the input transducer (demonstrated in Figure 1). The Crystal Stik is a new URS device developed to improve both the temporal and spatial resolution, of URS techniques [54]. The Crystal Stik operates with a broadband transducer with a centre frequency of 50MHz, so the measuring rate is much higher than AAS making it capable of tracking dynamic changes, sensitive to a narrower, yet relevant range of length scales. The Crystal Stik measures the time of flight and amplitude of the signal across a quartz buffer rod and then through the sample. This can be used to directly determine the speed of sound, whilst reduction in the amplitude of the return signal indicates the acoustic attenuation due to the medium. Increased attenuation may be due to acoustic scattering events and can be used to calculate the clear point and cloud point of crystallisation, measure temperature precisely and monitor dynamic aggregation processes.

This study compares the particle size distribution of aggregating casein micelles at their iso-electric point through DLS and the inversion of ultrasound spectra obtained using AAS. These two systems are complimentary and the use of different measurement techniques can yield more information about the model system. The inversion of the ultrasound spectra allows particle fractions of different length scales to be fit independently, meaning the PSD and relative volume fraction can be resolved for populations of small particle sizes co-existing with populations of larger particles in an aggregated state. This is achieved through a series of in-situ measurements performed under shear as opposed to the static DLS measurements. The aggregation kinetics around the isoelectric point are then monitored using turbidity and Ultrasound Reflectance Spectroscopy.

Materials and Methods

To provide a model system of bovine milk, 0.8 % (w/w) casein dispersions were prepared by dissolving 4 g of micellar casein isolate (Arla Foods a.m.b.a., Denmark) into 500 mL of 0.1 M NaOH (Fluka, USA) solution. Micellar casein isolate was produced through membrane filtration fractionation to isolate casein micelles in their micellar state, before up concentrating and spray drying. The concentration of casein used in this study was selected to give the same volume fraction of casein present once hydrated as in bovine milk (~2-3% w/w). The initial pH of the NaOH solution was 13, upon complete addition and dispersion of the micellar casein, the pH was measured as 11.3. The pH of the solutions was then adjusted using either 1 M hydrochloric acid (Fluka, USA) and/or 1 M sodium hydroxide (Fluka, USA). MilliQ water (Millipore, USA) was used in all experiments.

The pH of the casein dispersions was altered using a potentiometric titrator (pH Stat) (Metrohm, Switzerland). The potentiometric titrator used consisted of a 902 Titrando unit and an 801 stirrer. The pH was controlled to within 0.001 pH unit using the Tiamo software. To determine the isoelectric point, the pH of the casein solution was adjusted to pre-determined end points using different pH intervals between 7 and 3 and the zeta potential at each point was determined using a Zetasizer Nano ZS (Malvern Instruments, UK). This process was then repeated by bringing the starting pH of the solution down to 3 and increasing the pH to the previously used endpoints via the addition of NaOH and the zeta potential again measured at each point. The volumes of acid and base required to reach each pH step were recorded. Samples were repeated in triplicate (n=3). Measurement temperatures were maintained at 25 °C throughout the titration and zeta potential measurements.

Once the isoelectric point was determined, the particle size was measured at ± 1 pH unit of the isoelectric point, at 0.5 pH unit intervals (which yielded the most accurate data), using both the Zetasizer and an Ultrasizer MSV (Malvern Instruments, UK) [52]. The size reported by the Zetasizer was an intensity distribution based on the volume of the scatterers. To determine the particle size distribution acoustically, an attenuation spectrum was measured using the Malvern Ultrasizer MSV a continuous and pulsed broadband technique to obtain a large dynamic frequency range. Typically, attenuation coefficients are determined which range from 0.1 to several hundred decibels per centimetre over the frequency range 1–120 MHz with an accuracy of better than 3.5% and velocity measured to within 0.01 %. The spectra may then be

inverted using an established single particle thermo-viscous acoustic scattering model ECAH which further uses multiple scattering theory to accommodate many-particle systems. For a full description see Povey [67].

In the ECAH model, differences in compressibility and thermal properties between particle and medium permit calculation of the excess attenuation due to the ensemble scattering of the particles which depends upon the concentration and particle size distribution. Inversion of the spectra can be obtained by using software such as Ultra-SCATTERER^{TM} (Felix ALBA Consultants, Inc) and volume fraction ϕ and radius of particles may be determined. Inversion of the spectra requires minimisation of residuals between model and experimental data across each measured frequency to predict a distribution of particle sizes and associated volume fractions. The mean particle size and volume fraction is then reported as the D_{43} diameter (nm).

Once the isoelectric point had been determined and the particle size trend around the isoelectric point had been measured, the dissolution and aggregation characteristics of the casein dispersions were monitored around the isoelectric point. Dissolution and aggregation were monitored using optical turbidity methods via an ASD12 turbidity probe attached to a Control 4000 system (OPTEK, Germany). The dissolution and aggregation characteristics were monitored concurrently with the Crystal Stik.

The Crystal Stik contains a 50 MHz transducer, a quartz buffer rod and an acoustic reflection plate. In this study it was used to determine the starting point of the aggregation and redistribution of the casein micelles as the pH was changed. The Crystal Stik was connected to a UT320 Pulser Receiver system (UTEX Scientific Instruments, Canada) and the output was monitored with a Wavesurfer 3034 oscilloscope (Teledyne Le Croy, France). During measurement, the temperature of the sample was controlled using a glass jacketed vessel filled with SilOil M40.165.10 Thermofluid (Huber, Germany) which was pumped from a Pilot One Ministat circulator (Huber, Germany). The temperature of the sample was monitored using a PT100 probe connected to the Ministat. All aggregation experiments were performed at 25 °C.

Results & Discussion

To measure the isoelectric point of micellar casein dispersions the pH of the solution was progressively lowered, and zeta potential measurements were measured at precise pH intervals. Firstly, a rough isoelectric point was determined, then subsequent finer pH steps were used to get a more precise measurement. The zeta potential was also measured starting from a pH below the isoelectric point with the pH being raised past the isoelectric point with addition of sodium hydroxide to measure the hysteresis. Figure 2 shows the zeta potential determination using 0.5 steps in pH for the 0.8 % casein dispersions. Steps of 0.5 were chosen as preliminary experiments that used pH steps of 0.2 and 0.33 pH were found to be too inconsistent close to the isoelectric point.

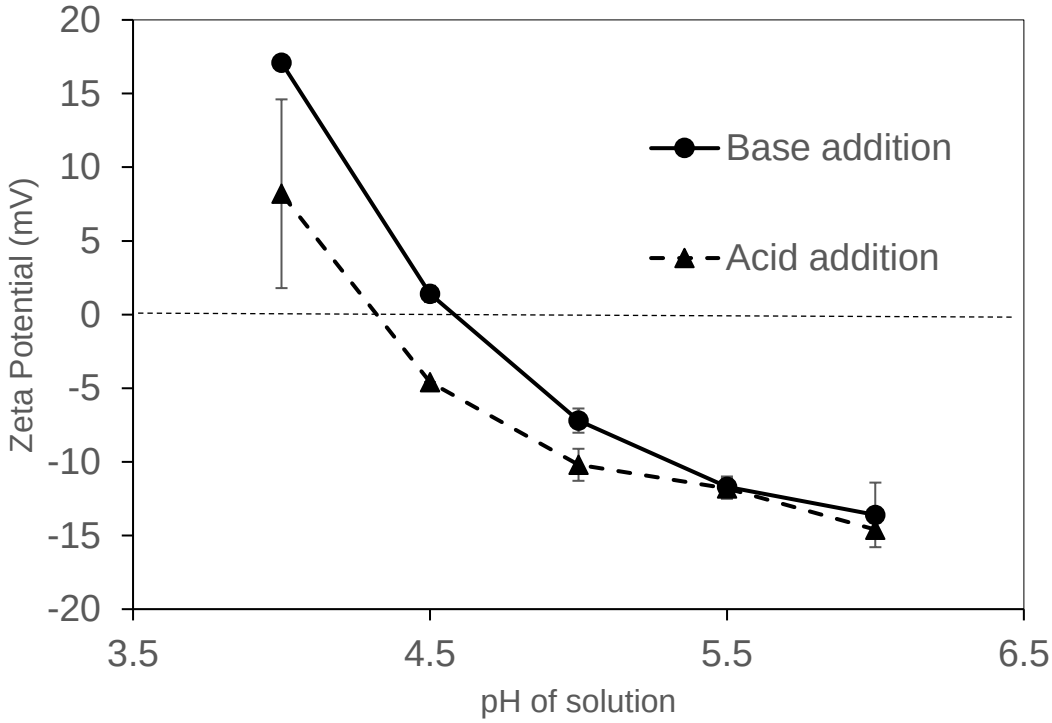

Figure 2: Effect of acidification and alkalisation on micellar casein dispersions. Change in zeta potential as a function of pH to determine the isoelectric point.

From this series of measurements, the average isoelectric point for the casein solution was determined to be 4.5 ± 0.2. For subsequent measurements a pH of 4.5 corresponds to measurements performed at the isoelectric point. It is interesting to note that the zeta potential on average is very negative at pH 5 but sharply transitions to positive at pH 4. It has been reported that the addition of between 0.1M to 0.6M NaCl can alter the zeta potential of casein micelles by between 1.6 mV and 9.4 mV [68]. The maximum possible concentration of NaCl present in the model system here, at pH 4, would be 0.1M. The presence of this concentration of salt could change the zeta potential by up to 1.6 mV which might explain the hysteresis seen in Figure 2 which increases as the NaCl concentration increases. However, given that the isoelectric point is similar to that reported in numerous studies [23,24] we can assume that the formation of salt is not affecting the formation of aggregates and the model system is behaving as expected.

Once the isoelectric point was determined, the average particle size of the casein dispersions was measured using Dynamic Light Scattering and Acoustic Attenuation Spectroscopy. The mean diameter and polydispersity index (PDI) determined using Dynamic Light Scattering is shown in Figure 3.

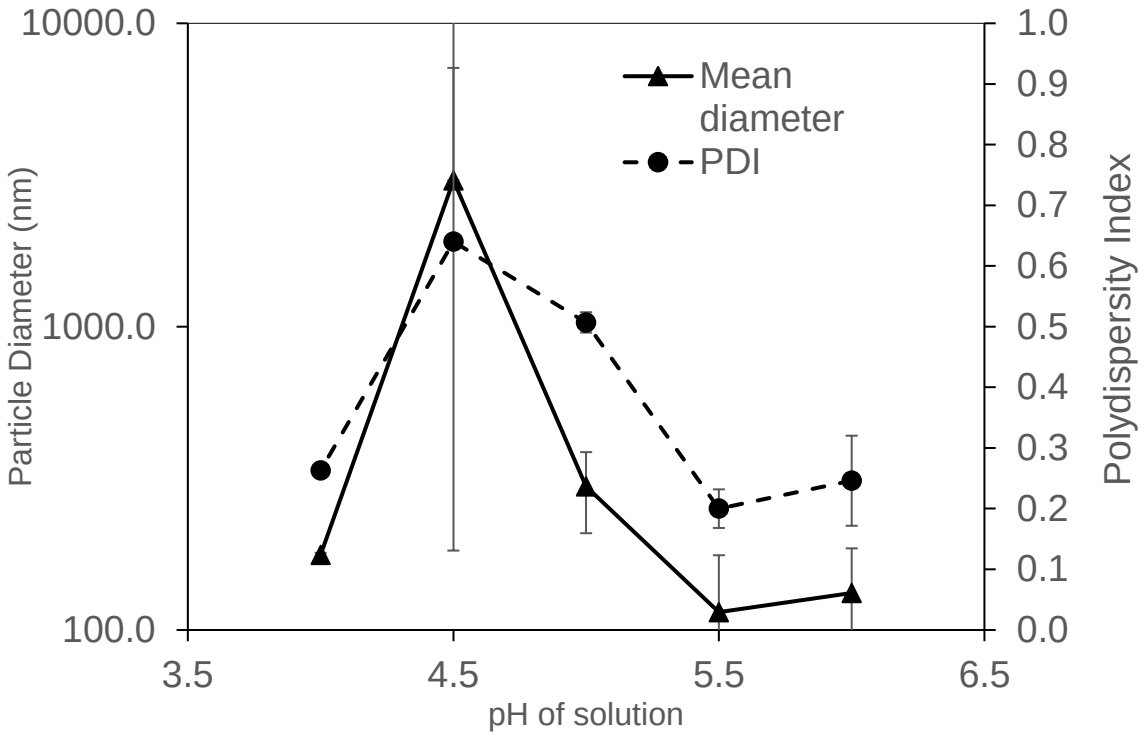

Figure 3: Effect of pH on the particle size distribution and polydispersity index (non-dimensional) of micellar casein dispersions around the isoelectric point, as determined with DLS.

As can be seen from Figure 3, the particle size below and above the isoelectric point show similar trends with a mean diameter of 146 ± 31 nm. The polydispersity index shows a comparable trend, with the PDI at pH 4, 5.5 and 6 showing a fairly monomodal distribution indicated by a polydispersity under 0.3. As expected at the isoelectric point, the reported polydispersity is high, and the mean diameter is much larger. This is due to the precipitation and aggregation process leading to a range of different sized, larger protein particles. As the aggregates are too large to be accurately measured by DLS, the reported values for PDI and diameter at the isoelectric point are purely indicative. The mean diameter and PDI begin to increase slightly at pH 5, relative to other pH values away from the isoelectric point. At pH 5 the zeta potential was measured as –7.2 mV which indicates a reduction in the surface charge, allowing the micelles to begin to aggregate. Outside of this region the steric and electrostatic repulsion provided by the surface charge will ensure the casein micelles are stable to aggregation and maintain a narrow size distribution.

Particle size distributions for the casein dispersions at different pH were then measured using Acoustic Attenuation Spectroscopy at different pH. The results of these measurements are shown in Figure 4.

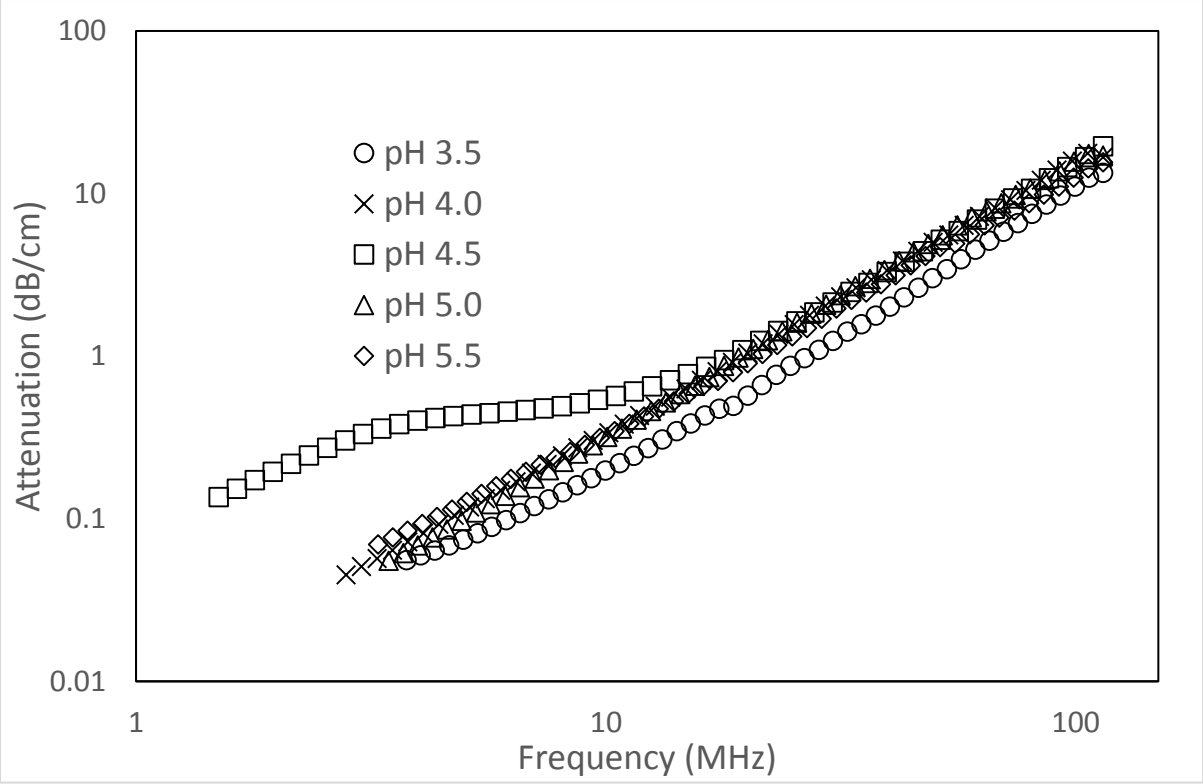

Figure 4: Acoustic attenuation spectra of micellar casein dispersions at different pH values around the isoelectric point of pH 4.5.

Figure 4 shows a consistent attenuation trend with frequency for all pH values either side of the isoelectric point. However, at the isoelectric point, there is a sharp increase in low frequency attenuation below 10 MHz. This is probably due to multiple scattering and solvent-protein relaxation effects arising from the aggregation of the micelles. The ECAH model was then fit to the attenuation spectra to determine the particle size distribution by minimising residual fits between data and model predictions. The parameters used in the inversion are shown in Table 1.

	Water	Casein
Ultrasound velocity (m s^{-1})	1497	1563
Density (kg m^{-3})	997	1076
Specific heat capacity (J kg^{-1} K^{-1})	4177	3818
Thermal conductivity (W m^{-1} K^{-1})	0.611	0.521
Thermal expansivity (K^{-1})	2.1×10^{-4}	7.5×10^{-4}
Attenuation exponent (MHz^{-2})	2.0	1.4
Attenuation coefficient (Np m^{-1})	0.023	4.02

Table 1. Physical properties of water and casein at 25℃ used in the numerical calculations to solve ECAH model [67,69–71].

A bimodal fit to the data indicated that two distributions were present. The peak diameters of these distributions are shown in Figure 5 and volume fractions are shown in Table 2 which includes details of D_{43} (nm) mean values and associated volume fractions (Φ) of the bimodal model fits relating to small and large micellar populations. Standard deviations of D_{43} are supplied in brackets.

	Small micelle		Large micelle		Mean volume fraction
pH	Φ	D_{43} /nm Mean (SD)	Φ	D_{43} /nm Mean (SD)	Φ
3.5	0.036	48 (4.5)	0.012	218 (23)	0.024
4	0.058	49 (4.5)	0.016	192 (17)	0.037
4.5	0.056	70 (6)	0.021	190 (15.5)	0.039
5	0.06	76 (6.5)	0.029	176 (15.5)	0.045
5.5	0.056	76 (6.5)	0.025	226 (22)	0.041

Table 2. Particle sizing of micellar casein dispersions at pH values around the isoelectric point determined from acoustic attenuation spectra.

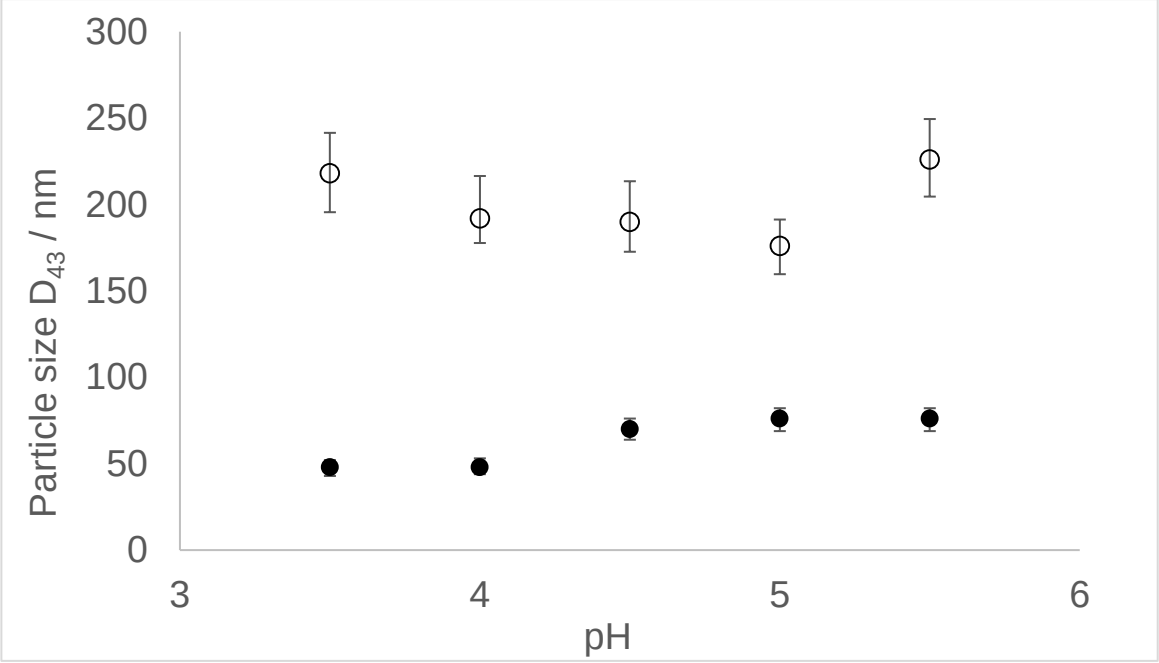

Figure 5: Effect of pH on mean D_{43} particle size distribution in micellar casein dispersions as a function of pH determined by Acoustic Attenuation Spectroscopy. Large micelle open circles and small micelle in solid dots.

The inversion of the attenuation spectra using the ECAH model indicated two distinct populations of particle size for each pH solution. Given that only casein micelles are present in the solution we refer to these populations as ‘large micelles’ and ‘small micelles’. It should be noted that during measurement in the Ultrasizer that continuous and appreciable agitation (500 rpm) takes place, to reduce thermal fluctuations. This provides sufficient shear in the sample to inhibit aggregation of micelles resulting in the reduced variation in PSD in micelle size which contrasts with the large PDI values reported in the DLS approach which do not undergo agitation during the measurement process. This aspect suggests that particle sizes are comparatively equivalent across all pH values covered but that steric and electrostatic stabilisation are the driving

process in aggregation. At pH 4.5, the isoelectric point, maximum aggregation occurs however, under high shear this process can be counteracted. This behaviour will be investigated further in future research.

Even though we are assuming a bimodal distribution, multiple populations of casein are expected given the broad size distribution normally reported for casein. From Figure 5, we can see a similar change in the size distribution with pH to that observed by Dynamic Light Scattering (Figure 3). The isoelectric point (around 4.5-5) shows a trend towards a reduction in diameter for the large micelle population yet shows an increase in the diameter of the small micelle population. This suggests that aggregation is occurring within the smaller population even with constant shear.

There are two things to note when comparing the results for the acoustic method of particle sizing to that obtained using Dynamic Light Scattering. Firstly, particle size predictions obtained using ultrasound spectroscopy are smaller than those measured by Dynamic Light Scattering, including at the isoelectric point, suggesting that the light scattering measurements potentially overestimate the proportion of larger particles. This may be a result of the comparison between DLS intensity to D_{43} volume PSD. Secondly, inversion of the acoustic spectrum using the ECAH model enabled determination of two dominant populations, most likely due to the applied shear, within the micelles while the light scattering measured monomodal distributions for all solutions outside the isoelectric point.

Following the particle size determination of the casein dispersions, the solution kinetics were observed using acoustic and optical means. Turbidity data was measured simultaneously with the attenuation data provided by the Crystal Stik. The initial NaOH solution was measured as a control and then the micellar casein isolate powder was added to the solution and the sample allowed to stabilise as complete dissolution occurred. The pH of the solution was then changed to 4.5 by the addition of 1 M HCl to aggregate the micelles. The solution was left to stabilise before the pH was changed back to 5.5 with 1 M NaOH solution to redistribute the micelles. Figure 6 presents the turbidity data along with Crystal Stik data for the casein dispersions at different pH over time.

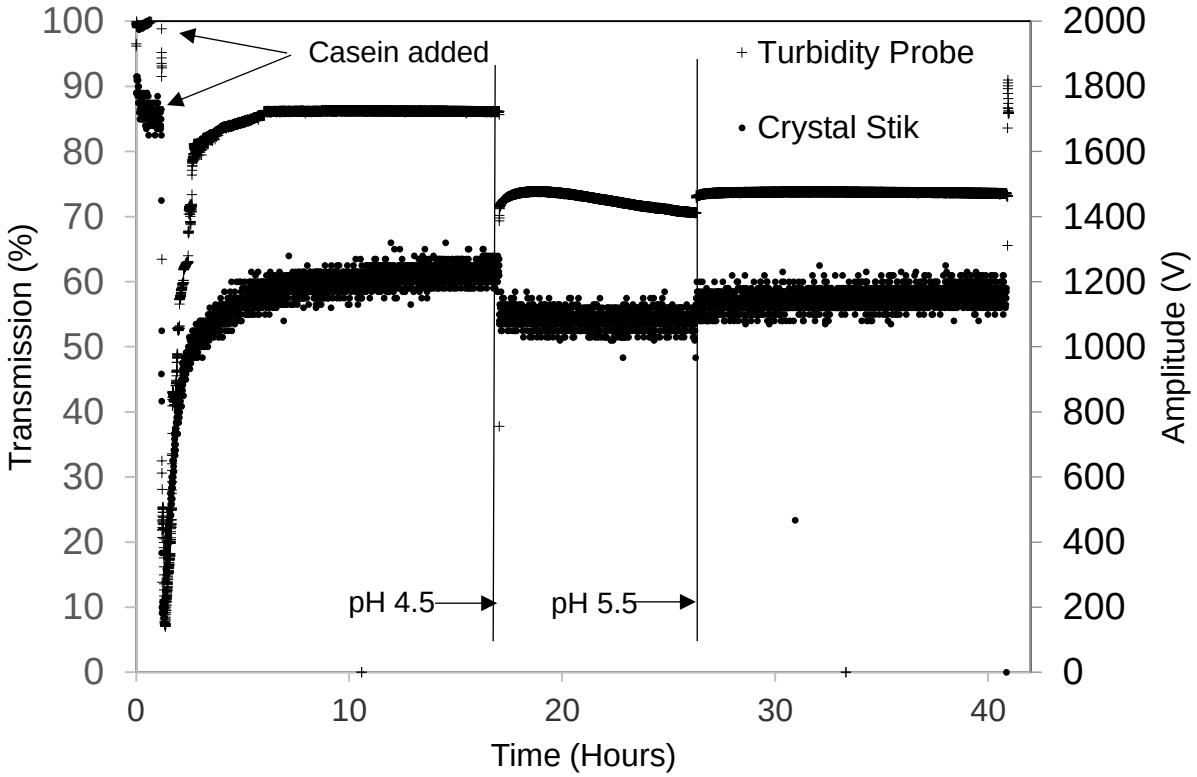

Figure 6: Changes in optical transmission and acoustic amplitude in dispersions of micellar casein as the pH is changed over time, measured with a turbidity meter and Crystal Stik respectively.

Due to the long experimental run time, the data appears to be following identical trends between the two techniques. To determine if one technique has a temporal advantage it is necessary to focus on one of the transition points in Figure 6. Figure 7 focusses on the point where the pH is changed to 4.5 and the isoelectric point is reached for the solution.

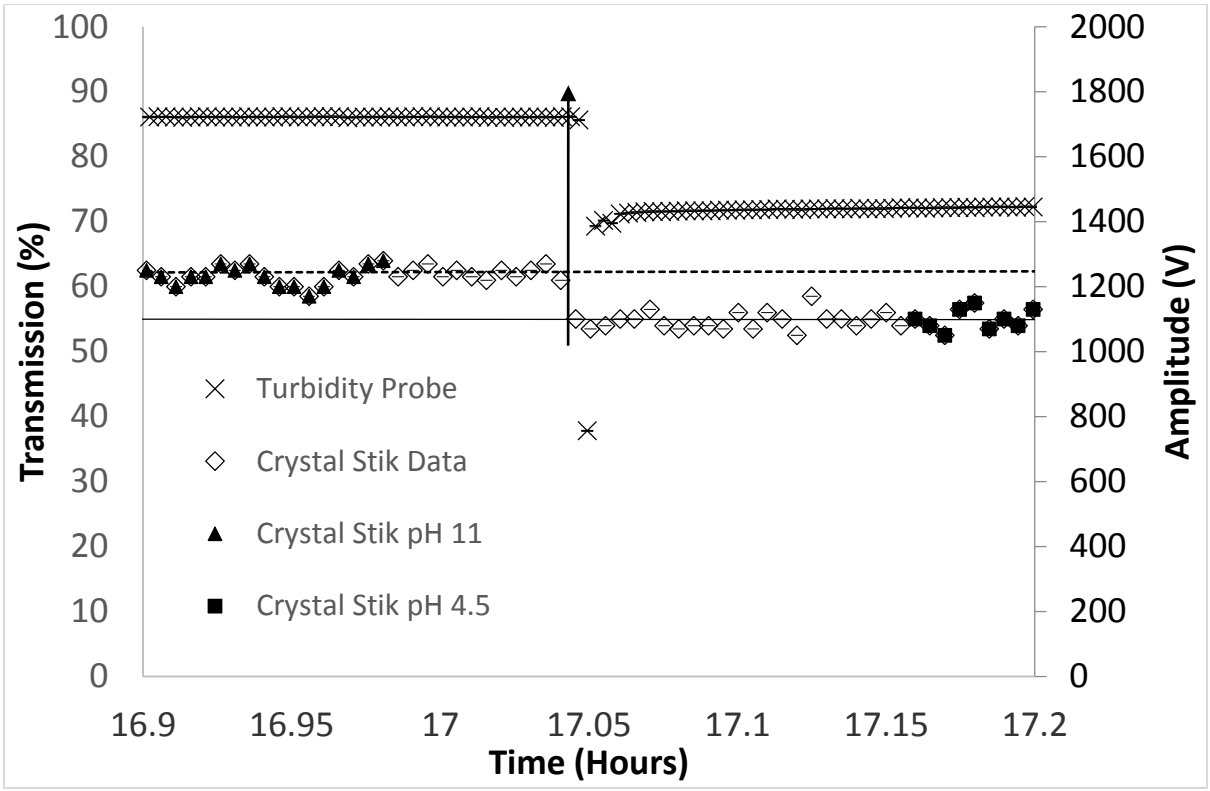

Figure 7: Changes in optical transmission and acoustic amplitude in dispersions of micellar casein, during transition to the isoelectric point of pH 4.5.

From Figure 7 it is evident that the temporal resolution for both techniques is similar. Linear trend lines were fitted to the Crystal Stik data either side of the transition region to determine the point at which the acoustic technique measures the transition (indicated with an arrow). The frequency of the measurements is not the limiting factor here as the both techniques can collect sufficient data points per unit of time to make a comparison.

The amplitude fluctuates slightly for the Crystal Stik data close to the isoelectric point but not for the turbidity probe. The ultrasound probe may be detecting fluctuations in the concentration of micelles in the liquid column. There may be reversible redistribution and aggregation occurring as the pH is changing to 4.5 and subsequently to 5.5 that the turbidity probe is unable to measure. These results will require further experimentation with additional dairy powder systems to confirm. The changes in acoustic attenuation measured by the Crystal Stik at 50 MHz will arise due to scattering and relaxation effects over the entire size range of casein micelles whereas the Turbidity Probe will only respond to scattering from larger particles, approximately above 80 nm.

Conclusion

Ultrasound techniques are economic, non-destructive and can work with industrially relevant compositions allowing for accurate in situ measurements. The study has shown that the Acoustic Attenuation spectra can be inverted to produce a particle size distribution and volume fraction for co-existing populations of particles, close to the isoelectric point of a protein dispersion. Dynamic changes in a dispersing, aggregating

and redistributed system can be effectively monitored with Ultrasound Reflectance Spectroscopy. The trends observed with the acoustic based techniques agree with those obtained by optical techniques, DLS and Turbidity measurements respectively.

Future work will focus on examining more complex dairy powder systems which include casein. A similar toolkit of ultrasound and optical methods will be used to determine what are the most important factors and constituents in dairy powders that affect the rehydration rates and aggregation of reconstituted dairy systems.

References

1. Lucey JA. Cultured dairy products: An overview of their gelation and texture properties. Int J Dairy Technol. 2004;57(2-3):77-84. doi:10.1111/j.1471-0307.2004.00142.x
2. Havea P, Singh H, Creamer LK. Heat-induced aggregation of whey proteins: Comparison of cheese WPC with acid WPC and relevance of mineral composition. J Agric Food Chem. 2002;50(16):4674-4681. doi:10.1021/jf011583e
3. González-Martínez C, Becerra M, Cháfer M, Albors A, Carot JM, Chiralt A. Influence of substituting milk powder for whey powder on yoghurt quality. Trends Food Sci Technol. 2002;13(9-10):334-340. doi:10.1016/S0924-2244(02)00160-7
4. Grunwald L, Petz M. Food processing effects on residues: Penicillins in milk and yoghurt. Anal Chim Acta. 2003;483(1-2):73-79. doi:10.1016/S0003-2670(02)01405-8
5. Aliste MA, Kindstedt PS. Effect of increasing pH on texture of full and reduced-fat cream cheese. Aust J Dairy Technol. 2005;60(3):225-230. http://www.scopus.com/inward/record.url?eid=2-s2.0-27744556698&partnerID=tZOtx3y1.
6. Hill AR, Irvine DM, Bullock DH. Precipitation and Recovery of Whey Proteins: A Review. Can Inst Food Sci Technol J. 1982;15(3):155-160. doi:10.1016/S0315-5463(82)72529-5
7. Breeding CJ, Marshall RT. Crystallization of butter oil and separation by filter-centrifugation. J Am Oil Chem Soc. 1995;72(4):449-453. doi:10.1007/BF02636087
8. Buldo P, Kirkensgaard JJK, Wiking L. Crystallization mechanisms in cream during ripening and initial butter churning. J Dairy Sci. 2013;96(11):6782-6791. doi:10.3168/jds.2012-6066
9. Kenny S, Wehrle K, Stanton C, Arendt EK. Incorporation of dairy ingredients into wheat bread: Effects on dough rheology and bread quality. Eur Food Res Technol. 2000;210(6):391-396. doi:10.1007/s002170050569
10. Hug-Iten S, Handschin S, Conde-Petit B, Escher F. Changes in Starch Microstructure on Baking and Staling of Wheat Bread. LWT - Food Sci Technol. 1999;32(5):255-260. doi:10.1006/fstl.1999.0544
11. Sato K. Crystallization behaviour of fats and lipids - A review. Chem Eng Sci. 2001;56(7):2255-2265. doi:10.1016/S0009-2509(00)00458-9
12. Hartel RW. Advances in Food Crystallization. Annu Rev Food Sci Technol. 2013;4(1):277-292. doi:10.1146/annurev-food-030212-182530
13. Puvanenthiran A, Williams RPW, Augustin MA. Structure and visco-elastic properties of set yoghurt with altered casein to whey protein ratios. Int Dairy J. 2002;12(4):383-391. doi:10.1016/S0958-6946(02)00033-X

14. Vercet A, Oria R, Marquina P, Crelier S, Lopez-Buesa P. Rheological properties of yoghurt made with milk submitted to manothermosonication. J Agric Food Chem. 2002;50(21):6165-6171. doi:10.1021/jf0204654
15. Horne DS. Casein interactions: Casting light on the black boxes, the structure in dairy products. Int Dairy J. 1998;8(3):171-177. doi:10.1016/S0958-6946(98)00040-5
16. Ruettimann KW, Ladisch MR. Casein micelles: structure, properties and enzymatic coagulation. Enzyme Microb Technol. 1987;9(10):578-589. doi:10.1016/0141-0229(87)90109-8
17. Holt C, Dalgleish DG. Electrophoretic and hydrodynamic properties of bovine casein micelles interpreted in terms of particles with an outer hairy layer. J Colloid Interface Sci. 1986;114(2):513-524. doi:10.1016/0021-9797(86)90437-6
18. Tuinier R, De Kruif CG. Stability of casein micelles in milk. J Chem Phys. 2002;117(3):1290-1295. doi:10.1063/1.1484379
19. Horne DS. A balanced view of casein interactions. Curr Opin Colloid Interface Sci. 2017;28:74-86. doi:10.1016/j.cocis.2017.03.009
20. Tran Le T, Saveyn P, Hoa HD, Van der Meeren P. Determination of heat-induced effects on the particle size distribution of casein micelles by dynamic light scattering and nanoparticle tracking analysis. Int Dairy J. 2008;18(12):1090-1096. doi:10.1016/j.idairyj.2008.06.006
21. Fox PF, Brodkorb A. The casein micelle: Historical aspects, current concepts and significance. Int Dairy J. 2008;18(7):677-684. doi:10.1016/j.idairyj.2008.03.002
22. Liu Y, Guo R. pH-dependent structures and properties of casein micelles. Biophys Chem. 2008;136(2-3):67-73. doi:10.1016/j.bpc.2008.03.012
23. Hofland GW, Van Es M, Van Der Wielen L a M, Witkamp GJ. Isoelectric Precipitation of Casein Using High-Pressure CO2. Ind Eng Chem Res. 1999;38:4919-4927. doi:10.1021/ie990136+
24. Moyer LS. Electrokinetic Aspects of Surface Chemistry VIII: The Composition of the Surface Film on Fat Droplets in Cream. J Biol Chem. 1940;133:29-39.
25. Dombrowski J, Dechau J, Kulozik U. Multiscale approach to characterize bulk, surface and foaming behavior of casein micelles as a function of alkalinisation. Food Hydrocoll. 2016;57:92-102. doi:10.1016/j.foodhyd.2015.12.022
26. Ahmad S, Piot M, Rousseau F, Grongnet JF, Gaucheron F. Physico-chemical changes in casein micelles of buffalo and cow milks as a function of alkalinisation. Dairy Sci Technol. 2009;89(3-4):387-403. doi:10.1051/dst/2009020
27. Huppertz T, Vaia B, Smiddy MA. Reformation of casein particles from alkaline-disrupted casein micelles. J Dairy Res. 2008;75(1):44-47. doi:10.1017/S0022029907002956
28. Horne DS. Casein micelle structure: Models and muddles. Curr Opin Colloid Interface Sci. 2006;11(2-3):148-153. doi:10.1016/j.cocis.2005.11.004
29. Zheng T, Bott S, Huo Q. Techniques for Accurate Sizing of Gold Nanoparticles Using Dynamic Light Scattering with Particular Application to Chemical and Biological Sensing Based on Aggregate Formation. ACS Appl Mater Interfaces. 2016;8(33):21585-21594. doi:10.1021/acsami.6b06903
30. Zhou C, Qi W, Lewis EN, Carpenter JF. Concomitant Raman spectroscopy and dynamic light scattering for characterization of therapeutic proteins at high concentrations. Anal Biochem. 2015;472:7-20. doi:10.1016/j.ab.2014.11.016

31. Stetefeld J, McKenna SA, Patel TR. Dynamic light scattering: a practical guide and applications in biomedical sciences. Biophys Rev. 2016;8(4):409-427. doi:10.1007/s12551-016-0218-6
32. Brandel C, Ter Horst JH. Measuring induction times and crystal nucleation rates. Faraday Discuss. 2015;179:199-214. doi:10.1039/c4fd00230j
33. Van Driessche AES, Van Gerven N, Bomans PHH, et al. Molecular nucleation mechanisms and control strategies for crystal polymorph selection. Nature. 2018;556(7699):89-94. doi:10.1038/nature25971
34. Li J, Yin Z, Ding Z, et al. Homogeneous nucleation of Al(OH)3 crystals from supersaturated sodium aluminate solution investigated by in situ conductivity. Hydrometallurgy. 2016;163:77-82. doi:10.1016/j.hydromet.2016.03.010
35. Hall D, Zhao R, Dehlsen I, et al. Protein aggregate turbidity: Simulation of turbidity profiles for mixed-aggregation reactions. Anal Biochem. 2016;498:78-94. doi:10.1016/j.ab.2015.11.021
36. Garcia VM, Rowlett VW, Margolin W, Morano KA. Semi-automated microplate monitoring of protein polymerization and aggregation. Anal Biochem. 2016;508:9-11. doi:10.1016/j.ab.2016.05.016
37. Zhou W, Chen H, Ou L, Shi Q. Aggregation of ultra-fine scheelite particles induced by hydrodynamic cavitation. Int J Miner Process. 2016;157:236-240. doi:10.1016/j.minpro.2016.11.003
38. Pisponen A, Mootse H, Poikalainen V, Kaart T, Maran U, Karus A. Effects of temperature and concentration on particle size in a lactose solution using dynamic light scattering analysis. Int Dairy J. 2016;61. doi:10.1016/j.idairyj.2016.06.006
39. Liang L, Zhen S, Huang C. Visual and light scattering spectrometric method for the detection of melamine using uracil 5′-triphosphate sodium modified gold nanoparticles. Spectrochim Acta - Part A Mol Biomol Spectrosc. 2017;173:99-104. doi:10.1016/j.saa.2016.08.049
40. Casanova F, Nogueira Silva NF, Gaucheron F, et al. Stability of casein micelles cross-linked with genipin: A physicochemical study as a function of pH. Int Dairy J. 2017;68:70-74. doi:10.1016/j.idairyj.2016.12.006
41. Langevin D, Raspaud E, Mariot S, et al. Towards reproducible measurement of nanoparticle size using dynamic light scattering: Important controls and considerations. NanoImpact. 2018;10:161-167. doi:10.1016/j.impact.2018.04.002
42. Xu R. Light scattering: A review of particle characterization applications. Particuology. 2015;18:11-21. doi:10.1016/j.partic.2014.05.002
43. Fischer K, Schmidt M. Pitfalls and novel applications of particle sizing by dynamic light scattering. Biomaterials. 2016;98:79-91. doi:10.1016/j.biomaterials.2016.05.003
44. Rai AK, Kumar A. Continuous measurement of suspended sediment concentration: Technological advancement and future outlook. Meas J Int Meas Confed. 2015;76:209-227. doi:10.1016/j.measurement.2015.08.013
45. Dorea CC, Simpson MR. Turbidity tubes for drinking water quality assessments. J Water, Sanit Hyg Dev. 2011;1(4):233. doi:10.2166/washdev.2011.058
46. Lambrou TP, Anastasiou CC, Panayiotou CG. A nephelometric turbidity system for monitoring residential drinking water quality. In: Lecture Notes of the Institute for Computer Sciences, Social-Informatics and Telecommunications Engineering. Vol 29 LNICST. ; 2010:43-55.

doi:10.1007/978-3-642-11870-8_4
47. Povey MJW. Applications of ultrasonics in food science - novel control of fat crystallization and structuring. Curr Opin Colloid Interface Sci. 2017;28:1-6. doi:10.1016/j.cocis.2016.12.001
48. Awad TS, Moharram HA, Shaltout OE, Asker D, Youssef MM. Applications of ultrasound in analysis, processing and quality control of food: A review. Food Res Int. 2012;48(2):410-427. doi:10.1016/j.foodres.2012.05.004
49. O'Brien RW, Cannon DW, Rowlands WN. Electroacoustic Determination of Particle Size and Zeta Potential. J Colloid Interface Sci. 1995;173(2):406-418. doi:10.1006/jcis.1995.1341
50. Povey MJW. Ultrasound particle sizing: A review. Particuology. 2013;11(2):135-147. doi:10.1016/j.partic.2012.05.010
51. Griffin WG, Griffin MCA. The attenuation of ultrasound in aqueous suspensions of casein micelles from bovine milk. J Acoust Soc Am. 1990;87(6):2541-2550. doi:10.1121/1.399047
52. Povey MJW, Golding M, Higgs D, Wang Y. Ultrasonic spectroscopy studies of casein in water. Int Dairy J. 1999;9(3-6):299-303. doi:10.1016/S0958-6946(99)00078-3
53. Buckin V. High-resolution ultrasonic spectroscopy. J Sensors Sens Syst. 2018;7(1):207-217. doi:10.5194/jsss-7-207-2018
54. Wade T, Beattie JK, Rowlands WN, Augustin M-A. Electroacoustic determination of size and zeta potential of casein micelles in skim milk. J Dairy Res. 1996;63(3):387. doi:10.1017/S0022029900031915
55. Dalgleish DG, Verespej E, Alexander M, Corredig M. The ultrasonic properties of skim milk related to the release of calcium from casein micelles during acidification. Int Dairy J. 2005;15(11):1105-1112. doi:10.1016/j.idairyj.2004.11.016
56. Wang Q, Bulca S, Kulozik U. A comparison of low-intensity ultrasound and oscillating rheology to assess the renneting properties of casein solutions after UHT heat pre-treatment. Int Dairy J. 2007;17(1):50-58. doi:10.1016/j.idairyj.2005.12.008
57. Dwyer C, Donnelly L, Buckin V. Ultrasonic analysis of rennet-induced pre-gelation and gelation processes in milk. J Dairy Res. 2005;72(3):303-310. doi:10.1017/S0022029905001020
58. Ferrer M, Alexander M, Corredig M. Changes in the physico-chemical properties of casein micelles during ultrafiltration combined with diafiltration. LWT - Food Sci Technol. 2014;59(1):173-180. doi:10.1016/j.lwt.2014.04.037
59. Chappellaz A, Alexander M, Corredig M. Phase separation behavior of caseins in milk containing flaxseed gum and κ-carrageenan: A light-scattering and ultrasonic spectroscopy study. Food Biophys. 2010;5(2):138-147. doi:10.1007/s11483-010-9154-3
60. Liu J, Alexander M, Verespej E, Corredig M. Real-time determination of structural changes of sodium caseinate-stabilized emulsions containing pectin using high resolution ultrasonic spectroscopy. Food Biophys. 2007;2(2-3):67-75. doi:10.1007/s11483-007-9032-9
61. Alba F, Crawley GM, Fatkin J, Higgs DMJ, Kippax PG. Acoustic spectroscopy as a technique for the particle sizing of high concentration colloids, emulsions and suspensions. Colloids Surfaces A Physicochem Eng Asp. 1999;153(1-3):495-502. doi:10.1016/S0927-7757(98)00473-7
62. Allegra JR, Hawley SA. Attenuation of Sound in Suspensions and Emulsions:

Theory and Experiments. J Acoust Soc Am. 1972;51(5B):1545. doi:10.1121/1.1912999
63. Kulmyrzaev A, Cancelliere C, McClements DJ. Characterization of aerated foods using ultrasonic reflectance spectroscopy. J Food Eng. 2000;46(4):235-241. doi:10.1016/S0260-8774(00)00070-4
64. McClements DJ. Ultrasonic characterisation of emulsions and suspensions. Adv Colloid Interface Sci. 1991;37(1-2):33-72. doi:10.1016/0001-8686(91)80038-L
65. Priego-Capote F, Luque De Castro MD. Analytical uses of ultrasound II. Detectors and detection techniques. TrAC - Trends Anal Chem. 2004;23(10-11):829-838. doi:10.1016/j.trac.2004.07.013
66. Tong J, Povey MJW. Pulse echo comparison method with FSUPER to measure velocity dispersion in n-tetradecane in water emulsions. Ultrasonics. 2002;40(1-8):37-41. doi:10.1016/S0041-624X(02)00088-4
67. Povey MJW. Ultrasonic Techniques for Fluids Characterization. Academic Press; 1997. doi:10.1016/B978-012563730-5/50005-2
68. Huppertz T, Fox PF. Effect of NaCl on some physico-chemical properties of concentrated bovine milk. Int Dairy J. 2006;16(10):1142-1148. doi:10.1016/j.idairyj.2005.09.011
69. Del Grosso VA, Mader CW. Speed of Sound in Pure Water. J Acoust Soc Am. 1972;52(5B):1442-1446. doi:10.1121/1.1913258
70. Vance S, Brown JM. Sound velocities and thermodynamic properties of water to 700 MPa and −10 to 100 °C. J Acoust Soc Am. 2010;127(1):174-180. doi:10.1121/1.3257223
71. Alba, F.; Higgs, D.; Jack, R.; Kippax P. Ultrasound spectroscopy: A sound approach to sizing of concentrated particulates. In: Handbook on Ultrasonic and Dielectric Characterization Techniques for Suspended Particulates. American Ceramic Society; 1998.

Competing interest statement

Powders were supplied by Arla Foods a.m.b.a Denmark. The authors have no competing interests to declare. This work was funded by: Ultrasonic propagation in complex media: correlated spatial distributions and multiple dispersed phases Professor Megan Povey: University of Leeds EP/M026310/1